PHYSICAL REVIEW B **86**, 201103(R) (2012)

Nonmonotonic Fermi surface evolution and its correlation with stripe ordering in bilayer manganites

Z. Sun,[1,2,*] Q. Wang,[1] J. F. Douglas,[1] Y.-D. Chuang,[3] A. V. Fedorov,[3] E. Rotenberg,[3] H. Lin,[4] S. Sahrakorpi,[4] B. Barbiellini,[4] R. S. Markiewicz,[4] A. Bansil,[4] H. Zheng,[5] J. F. Mitchell,[5] and D. S. Dessau[1,†]

[1]*Department of Physics, University of Colorado, Boulder, Colorado 80309, USA*

[2]*National Synchrotron Radiation Laboratory, University of Science and Technology of China, Hefei, Anhui 230029, People's Republic of China*

[3]*Advanced Light Source, Lawrence Berkeley National Laboratory, Berkeley, California 94720, USA*

[4]*Department of Physics, Northeastern University, Boston, Massachusetts 02115, USA*

[5]*Materials Science Division, Argonne National Laboratory, Argonne, Illinois 60439, USA*

(Received 20 October 2010; revised manuscript received 27 February 2012; published 6 November 2012)

Using angle-resolved photoemission spectroscopy, we have measured $La_{2-2x}Sr_{1+2x}Mn_2O_7$ over a wide doping range to study the correlation between Fermi surface nesting and stripes of charge and orbital degrees of freedom. We found that the Fermi surface nesting deviates from band calculations with a nonmonotonic behavior, and that one type of stripe is exclusively linked to long flat portions of nested Fermi surface, while the other type prefers to be commensurate with the real-space lattice but also may be driven away from this by the Fermi surface. Complementarily, for certain doping levels pressure from the stripe ordering also may drive the Fermi surface away from its preferred trend.

DOI: 10.1103/PhysRevB.86.201103 PACS number(s): 71.18.+y, 75.25.Dk, 75.47.Gk, 79.60.−i

Strong electron correlation effects of various kinds can yield nanoscale self-organizations of charges, spins, and orbitals, often forming stripelike patterns, with these patterns generally believed to be highly relevant for the exotic physical properties of many novel electronic materials, such as cuprates, manganites, nickelate, etc.[1–3] For example, in the family of bilayer manganites $La_{2-2x}Sr_{1+2x}Mn_2O_7$, various charge and orbital stripes have been observed over a wide doping range in the two-dimensional planes of MnO_6 octahedra[4–12] [see Fig. 1(a) for the crystal structure and Figs. 1(d) and 1(e) for typical cartoons of stripes]. It has been found that the scattering intensity associated with these modulations has a temperature dependence that very closely matches the electrical resistivity,[6,7,11,13] which suggests their relevance for the transport properties of these materials. On the other hand, the origin and nature of these stripe modulations are still quite controversial. In correlated electron systems, the underlying driving forces for these stripelike patterns and their importance for the novel physical properties have been the focus of modern condensed matter physics.

Despite their importance, little direct information exists about how stripe modulations alter or are altered by the electronic band structure, which can provide valuable details on the relationship of the itinerancy of mobile carriers and the ordering tendency of electron correlations. We attempt to approach this issue by investigating the band structure of $La_{2-2x}Sr_{1+2x}Mn_2O_7$. In these materials, stripes take place in the planes of MnO_6 octahedra, where the main physics occurs. Some stripes go in the diagonal direction[6–9] and some stripes run vertically along the in-plane Mn-O bonds.[10–12] In this Rapid Communication, we refer to them as D (diagonal) and V (vertical, although they can of course also be horizontal) types of stripes, respectively. The top view of an MnO_2 plane in Fig. 1(d) sketches a typical illustration for the famous D type of stripes, termed a CE stripe,[14] in $LaSr_2Mn_2O_7$. Figure 1(e) shows the top view of the modulation of MnO_6 octahedra, revealing the (0.3,0,1) V stripe in $La_{1.2}Sr_{1.8}Mn_2O_7$.[12] The periodicities and local structures of D and V types of stripes vary with doping.[4–12] The diversity of these stripes, together with the complex phase diagram [Fig. 1(b)], make $La_{2-2x}Sr_{1+2x}Mn_2O_7$ an excellent playground for studying the interplays between electronic band structures and stripes.

Following the pictures of charge density waves (CDWs) or spin density waves (SDWs), we look for the connection between Fermi surface topology and the stripe modulation periodicity in this material. We note that the strong electron correlation in $La_{2-2x}Sr_{1+2x}Mn_2O_7$ is strikingly different from the dominant itinerancy in the traditional CDW and SDW systems. As will be shown later, unusual properties arise in these materials with marked contrast to the classic CDWs and SDWs. The Fermi surface of $La_{2-2x}Sr_{1+2x}Mn_2O_7$ is dominated by one electronlike pocket (black) centered at the Γ point and two holelike pockets (green) around the zone corners[15] [see Fig. 1(c)]. The straight segments near the zone boundary are the bonding (solid green) and the antibonding (dashed green) portions of Fermi surface of bilayer-split bands that arise from the coherent hopping between the two neighboring MnO_2 planes per unit cell.[16,17] The bonding portions of the Fermi surface are straighter than the antibonding ones, so we expect these states to be more important for any ordering tendencies—an expectation which is borne out in our experiments. Superimposed on the Fermi surface are nesting vectors for both the diagonal or D stripes (blue) and the vertical or V stripes (red). Whether these nesting vectors match the scattering vectors observed from x-ray and neutron scattering is not yet known, with this information critical for reaching an understanding of the charge and orbital ordering patterns.[18,19] We used angle-resolved photoemission spectroscopy (ARPES) to measure these Fermi surface k vectors. As we will show, the correlation between stripes and Fermi surface nesting depends upon the specific stripe scattering q vectors and Fermi surface k vectors, which in turn

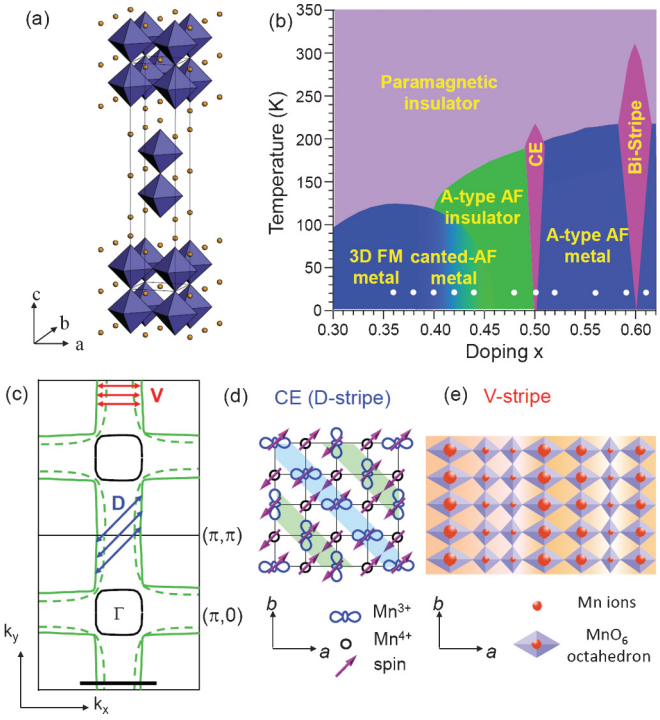

FIG. 1. (Color online) (a), (b) Crystal structure and phase diagram of $La_{2-2x}Sr_{1+2x}Mn_2O_7$. The blue blocks are MnO_6 octahedra. The complicated interactions yield a diversity of metallic, insulating, paramagnetic, ferromagnetic (FM), and antiferromagnetic (AF) states. At $x = 0.50$ and $x = 0.60$, the material is an insulator with CE-type and bi-stripe long range charge and orbital ordering, respectively (see Refs. 5 and 9). White dots indicate temperature and doping levels considered here. (c) A schematic Fermi surface plot of $La_{2-2x}Sr_{1+2x}Mn_2O_7$ shows holelike bonding (solid green) and antibonding (dashed green) portions of bilayer-split bands, as well as the electronlike zone center pocket. The arrows indicate two types of nesting vectors. As discussed in the text, they correspond to "vertical" (red) and "diagonal" (blue) stripes. (d) Top view of CE ordering in MnO_2 planes, which is a specific case of diagonal stripes. (e) Top view of short range (0.3,0,1) vertical stripes in the $x = 0.40$ compound.

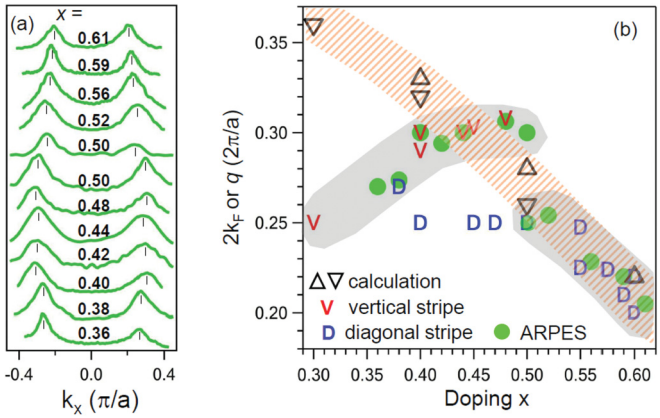

FIG. 2. (Color online) (a) Zone face MDCs [taken along the black line in Fig. 1(c)] at the Fermi level for various doping levels showing a nonmonotonic evolution with doping. For $x = 0.50$, two different nesting vectors were detected using s- and p-polarized light. (b) Compilation of experimental data and a comparison to theoretical calculations as a function of doping. V's and D's represent the "vertical stripe" and "diagonal stripe" ordering from scattering experiments (Refs. 6–12). We note here that the D values are the projections of D vectors to the (0,0)-$(\pi,0)$ direction. The gray shaded area shows the experimental trend determined by ARPES and x-ray scattering. Band theory results are shown as triangles with a hatched area indicating the general trend. Down triangles are from Ref. 19; up triangles are our own calculations. Solid green circles are ARPES data of the bonding bands or the nonbilayer split bands, taken from (a).

depends upon the doping levels. In addition, the experimental measurements of these vectors strongly deviate from band calculations.

The single crystals were grown using the traveling-solvent floating zone method as described elsewhere,[13] with a doping uncertainty of less than 0.01 or better. We have used ARPES to measure many samples with various doping levels, and the spectroscopic differences are clear and highly repeatable. For example, Refs. 16 and 20 on $x = 0.38$ samples show a consistent nesting behavior, while Refs. 18 and 21 exhibit a similar behavior for the $x = 0.40$ compound. Our experiments were performed at beamlines 7.0.1, 10.0.1, and 12.0.1 of the Advanced Light Source, Berkeley using Scienta electron spectrometers. All data shown here were taken in a vacuum of better than 3×10^{-11} Torr. Samples with various doping levels were cleaved *in-situ* and measured at 20 K. We took advantage of the ability to deconvolve bilayer splitting in these materials,[16] enabling much more careful studies of the Fermi surface nesting vectors. For the $x = 0.50$ sample we found that p-polarized light allowed us to observe the longer nesting vector and s-polarized light the shorter nesting vector (see Fig. 2). This suggests a difference of orbital symmetry for the different electronic states, the details of which will be described in a future publication. Band calculations were performed within the all-electron full-potential Korringa-Kohn-Rostoker and linearized augmented plane-wave methods using a rigid-band model. These calculations were described in Ref. 17 and provide a theoretical baseline for the experimental data, and the results [see Fig. 2(b)] show a doping behavior consistent with intuition. The band calculations focus on the itinerant electronic systems at low temperature, without charge and orbital orderings incorporated.

Figure 2(a) shows ARPES momentum distribution curves (MDCs) at the Fermi level taken along the black cut in Fig. 1(c) for various doping levels, which serve to allow a direct and rapid comparison of the Fermi surface nesting vectors. Because the Fermi surfaces are parallel throughout a large portion of the Brillouin zone, this particular cut is similar to many others. Different photon energies were used to emphasize the most relevant portion of the data, that is, the bonding bands (in the presence of bilayer splitting band[16]) or the degenerate band (when the splitting between bonding and antibonding bands disappears, which occurs at higher doping levels).[17] The separation of the double peaks is a measure of the nesting vectors. These nesting vectors, $2k_F$, are plotted in Fig. 2(b) (green circles) as a function of doping level. They have a large value $2k_F \sim 0.3(2\pi/a,0)$ for intermediate dopings $x \sim 0.40$–0.50, with noticeably smaller values at both higher and lower dopings. Such a nonmonotonic evolution with doping is unexpected from electronic structure

theory [red hatched region—up triangles (our calculations) and down triangles].[19] In general, the theoretical and experimental data show an excellent match for $x > 0.50$, including both the overall magnitudes and the slope of the trends. For $0.40 < x < 0.50$ the overall magnitudes of the vectors are roughly comparable, but we notice that the doping trend is different—the experimental data shows a nearly flat trend with reduced doping while the theory clearly continues to increase. This disagreement is more pronounced for $x < 0.40$, where the trend in the experimental data reverses.

Using ARPES, Chuang *et al.* first pointed out the correlation between the vertical stripes and the Fermi surface nesting (bonding band), for the $x = 0.40$ sample they studied had a separation in k space very similar to the q vectors of the vertical stripes.[18] This agreement can be seen in Fig. 2(b), where for $x = 0.40$ both the green circle (ARPES $2k_F$) and the red V (q vector from x-ray scattering) have the same magnitude, $\sim 0.3(2\pi/a)$.[12,18] In fact, Fig. 2(b) shows that the observed V vector very closely matches the measured Fermi surface nesting vector $2k_F$ over the entire range where this comparison can be made. For $x < 0.50$, an x-ray scattering experiment with even finer doping steps has been performed[22] which yields a result consistent with our ARPES measurements. Because of the unusual nonmonotonic behavior deviating from band calculations, it is extremely unlikely for the connections between Fermi surface nesting and vertical stripe periodicity to be a coincidence. In the absence of a clear real-space mechanism for this behavior, we argue that the V stripe modulations are intrinsically locked to and driven by the nesting properties of the Fermi surface, having an analogy with classic CDWs.

The clear correlation between the two different types of experiments over so large a doping range also indicates that the Fermi surfaces measured by the surface-sensitive ARPES technique are representative of the bulk, since they agree so well with the bulk-sensitive scattering data. The fact that the two completely different types of spectroscopies (scattering and ARPES) give such a close agreement indicates that they must be returning the correct values, and that the band calculation misses some ingredients. Such a failure of the band calculations to get the correct evolution of the Fermi surface with doping is highly unusual.

A couple of options are available to explain the disagreement found here. In these and other correlated electron systems, it is very common that one has to do with the strong (and potentially intrinsic) inhomogeneity, whereas the band calculations were done for a homogeneous system. Theoretical calculations have shown that such inhomogeneity may have strong and unexpected consequences on the electronic structure.[1] The drastic deviations of the Fermi surface from their theoretical values for $x < 0.40$ is relevant to the fact that there are clear differences in other physical parameters of the samples with $x < 0.39$ compared to those with $x = 0.40$ or greater.[16,20] In particular, by observing a metallic Fermi edge above T_c where the samples are globally insulating, we recently showed the coexistence of metallic and nonmetallic regions for $x < 0.39$,[20] which can be interpreted as arising from a phase separation into hole-rich and hole-poor regions. This evidence for phase separation is not apparent in samples with $x > 0.40$.[18,21] Such a phase separation may allow the electron count to match the chemical doping level, even while the Fermi surface deviates from Luttinger's homogeneous value. Additionally, orbital degrees of freedom may play an important role in shifting spectral weight from one set of orbitals to another. Band calculations suggest that the proportion of $d_{x^2-y^2}$ and $d_{3z^2-r^2}$ states in these bands varies with energy and momentum, and that the mixing of these states in the bonding band is significant.[17,23] Some experiments have suggested that, for $x < 0.50$, doping hole carriers removes electrons mainly of $d_{3z^2-r^2}$ character, while the electron count of $d_{x^2-y^2}$ orbital is less modified.[24,25] Such a possibility suggests that the additional $d_{3z^2-r^2}$ orbital can act as a charge "reservoir" or "lever" to enable the bonding band to follow tendencies or preferences other than those expected from the rigid doping model in band calculations.

In addition to the connection between the ARPES nesting vectors $2k_F$ and the V vectors, a similar connection exists between the periodicities of D stripes and the ARPES nesting vectors for certain doping levels, though not for all doping levels. The most famous D stripe modulation is the CE ordering at the commensurate doing level $x = 0.50$, which includes the modulation of the charge, spin, orbital, and lattice degrees of freedom in real space [Fig. 1(d)] originated by Goodenough in 1955.[14] This real-space modulation corresponds to a relatively short vector in k space: $q = (0.25,0.25,0)$ in units of 2π/a. A real-space picture has also been given for bi-stripes at $x = 0.60$, which should give a diagonal $q = (0.20,0.20,0)$, which is very close to the observed value of $(0.21,0.21,0)$.[6,9] The doping dependence of the observed D stripe q vectors shown here is quite generic to the cubic and single-layer families of the manganites. Away from $x = 0.50$, the q vectors of D stripes remain fixed at $(0.25,0.25)$ in the lightly underdoped regime ($x = 0.40$–0.50), while in the overdoped regime ($x = 0.50$–0.60) they decrease approximately linearly with doping x [blue D's in Fig. 2(b)]. When the q vectors of D stripes deviate from the commensurate value $(0.25,0.25,0)$ outside the range of $x = 0.40$–0.50 doping, we find that they closely match the Fermi surface nesting vectors $2k_F$. This is observed between $x = 0.50$ and 0.60 as well as for the one point $x = 0.38$ in the underdoped region. Apparently the D stripe q vectors either lock in commensurately with the real-space lattice or they closely track the Fermi surface.

In the purely real-space picture for the D stripes, the linear variation of the q vector with doping for $x > 0.50$ can be imagined as a microscopic mixture of the two fixed phases, e.g., CE ordering at $x = 0.50$ and bi-stripe ordering at $x = 0.60$, similar to the model proposed for cubic manganites by Chen *et al.*[26] In this picture for intermediate compositions one will expect to either observe two sets of diffraction peaks (one from each of the fixed phases) with a varying intensity ratio determined by the doping x through the lever rule, or, for an extremely fine mixture, a single broad peak. In contrast, a single sharp peak is observed[27] and the higher diffraction harmonics are very weak, indicating that the structural distortions are nearly sinusoidal.[28] This, as well as optical conductivity[29] and transport[30] experiments and theory,[31] are more consistent with a CDW-like picture which has an important or dominant k-space aspect to it. Figure 2(b) shows that for $x > 0.50$, the band calculations, Fermi surface nesting vectors, and q vectors of D stripes in the

bilayer manganites match each other, giving a microscopic justification for the CDW-like nature of the incommensurate D stripes—the D stripe energies in the incommensurately doped regime are lowered by forming a single CDW-like structure with a q vector which varies with electron count and thus approximately matches the Fermi surface nesting vectors. Though there is less information about the Fermi surfaces for the other families of manganites, it is reasonable to expect that this picture will generalize.

Between $x = 0.40$ and 0.50 the D stripe q vectors become locked to the commensurate value $q = (0.25,0.25,0)$, indicating the returned dominance of the real-space driving force for the D stripes in this doping range. It is therefore not surprising that here the Fermi surface becomes nested by the competing V stripes. The possibility for microscopic phase separation should be especially strong in this doping region, with small patches of CE order coexisting within the electron-rich region.[28,32] Alternately, a pseudo-CE type of behavior is possible, in which the Mn^{4+} sites become filled with extra d_{z^2} electrons.[33]

At the still lower doping level $x = 0.38$ a very interesting phenomenon occurs—the D stripe q vector is again pulled away from its commensurate value of $q = (0.25,0.25,0)$ while there is a concomitant downward movement of the Fermi surface nesting vector away from the band calculation value. With these shifts the measured D vector and ARPES nesting vector exactly match at $q \sim 2k_F \sim (0.27,0.27,0)$. The agreement here is unlikely to be a coincidence and suggests strong positive feedback—the energy gain for nesting the D stripe q vector pulls both the Fermi surface and the D stripe away from their doping trends and makes them match. This is clear evidence of a Fermi surface crossing being modified so as to more strongly nest a charge and orbital modulation. Note that in this doping range there are other pieces of Fermi surface and/or localized states which are available to accommodate electrons displaced by the movement of the bonding Fermi surfaces. Moreover, it would be interesting to see if scattering measurements could track the D vector to doping levels of $x = 0.34$ or below. Within the current picture we would expect this vector (if it exists) to return to values near $q = (0.25,0.25,0)$, as opposed to continuing to grow to larger values.

At $x = 0.38$, one may also wonder how the D stripes, which are typically observed only above T_c, can feed back to a Fermi surface topology measured at low temperature in the metallic regime. We discuss two explanations for this. First, we note that theoretical studies by Johannes and Mazin argue that the states away from E_F also contribute greatly to the formation of CDWs.[34] Additionally, we consider the possibility of dynamic stripes existing below T_c,[35] which can feed back to the Fermi surface nesting and the charge and orbital ordering at high temperature, while above T_c static stripes (which dominate or are necessary for most spectroscopies) exist.

The close connection between Fermi surface nesting vectors and the charge and orbital modulations is reminiscent of CDW and SDW pictures, in which the modulations of charge and spin degrees of freedom are driven by the Fermi surface topology. We have shown that the orbital degrees of freedom are involved in a similar scenario, in which Fermi surface nesting is responsible for the formation of orbital modulations. Although this picture is reminiscent of a CDW-like picture, we note that the physics is much richer than the classic CDW, including unusual temperature dependence and unexpected high-energy scales. For example, scattering measurements indicate that the V stripes exist up to the order of 500 K.[22] From this we can imagine a BCS weak coupling CDW gap $\triangle = 1.76k_BT_c \sim 75$ meV, with the main dispersive band reaching this energy scale. In contrast, we find gaps on the scale of hundreds of meV as well as broad energy distribution curve (EDC) peaks which are centered at even higher binding energies [see Fig. 3(a) for an example from the $x = 0.40$ material], suggesting the cooperation of the stripe or CDW physics with another higher-energy scale such as polarons, Mott, or orbital physics.[15,21] The large energy

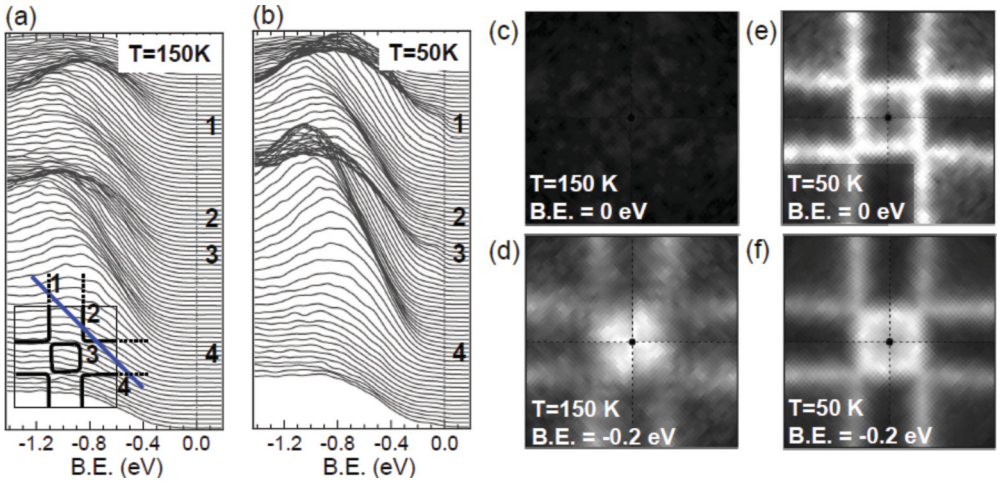

FIG. 3. (Color online) (a), (b) Stacked EDCs of $x = 0.40$ compound along the blue cut in the inset, taken at 150 and 50 K, respectively, showing the change of spectral weight. In the inset of (a), only the electronlike pocket and holelike bonding pockets are shown. (c)–(f) Spectral intensities at constant energy across the first Brillouin zone. (c) and (d) are at 150 K and (e) and (f) at 50 K, while (c) and (e) are at E_F and (d) and (f) are at 0.2 eV below E_F. (c)–(e) have an identical gray scale while the spectral weight in (f) was scaled down by a factor of 4 to prevent saturation.

scale gaps the entire Fermi surface [Fig. 3(c)] and drives the material insulating, though there is still a clear underlying k dependence at deeper energies [Fig. 3(d)], implying that the electrons are still delocalized in Bloch-like states. At low temperature, where the energy gain from electron itinerancy driven by double-exchange physics[36,37] begins to take over, the stripes dissolve and electronic states begin to leak into the gaps [Figs. 3(b), 3(e), and 3(f)].

The authors thank T. Devereaux, K. Gray, D. Reznik, D. N. Argyriou, and S. Rosenkranz for helpful discussions. This work was supported by the US National Science Foundation under Grant No. DMR 1007014. The Advanced Light Source (ALS) is supported by the Director, Office of Science, Office of Basic Energy Sciences, of the US Department of Energy under Contract No. DE-AC02-05CH11231. The theoretical work is supported by the US Department of Energy Contract No. DE-FG02-07ER46352, and benefited from the allocation of supercomputer time at the NERSC and the Northeastern University's Advanced Scientific Computation Center (ASCC). It is also supported by Grant No. DE-AC03-76SF00098 for theory support at the ALS. Z.S. acknowledges the National Natural Science Foundation of China (Grant No. 11174264). Argonne National Laboratory, a US Department of Energy Office of Science Laboratory, is operated under Contract No. DE-AC02-06CH11357.

*zsun@ustc.edu.cn

†dessau@colorado.edu

[1] E. Dagotto, Science **309**, 257 (2005).

[2] J. Zaanen, Science **286**, 251 (1999).

[3] V. J. Emery *et al.*, Proc. Natl. Acad. Sci. USA **96**, 8814 (1999).

[4] J. F. Mitchell *et al.*, J. Phys. Chem. B **105**, 10731 (2001).

[5] H. Zheng, Qing'An Li, K. E. Gray, and J. F. Mitchell, Phys. Rev. B **78**, 155103 (2008).

[6] Qing'An Li, K. E. Gray, S. N. Ancona, H. Zheng, S. Rosenkranz, R. Osborn, and J. F. Mitchell, Phys. Rev. Lett. **96**, 087201 (2006).

[7] J. Q. Li, C. Dong, L. H. Liu, and Y. M. Ni, Phys. Rev. B **64**, 174413 (2001).

[8] D. N. Argyriou, J. W. Lynn, R. Osborn, B. Campbell, J. F. Mitchell, U. Ruett, H. N. Bordallo, A. Wildes, and C. D. Ling, Phys. Rev. Lett. **89**, 036401 (2002).

[9] T. A. W. Beale *et al.*, Phys. Rev. B **72**, 064432 (2005).

[10] M. Kubota *et al.*, J. Phys. Soc. Jpn. **69**, 1986 (2000).

[11] L. Vasiliu-Doloc *et al.*, J. Appl. Phys. **89**, 6840 (2001).

[12] B. J. Campbell, R. Osborn, D. N. Argyriou, L. Vasiliu-Doloc, J. F. Mitchell, S. K. Sinha, U. Ruett, C. D. Ling, Z. Islam, and J. W. Lynn, Phys. Rev. B **65**, 014427 (2001).

[13] J. F. Mitchell, D. N. Argyriou, J. D. Jorgensen, D. G. Hinks, C. D. Potter, and S. D. Bader, Phys. Rev. B **55**, 63 (1997).

[14] J. B. Goodenough, Phys. Rev. **100**, 564 (1955).

[15] D. S. Dessau, T. Saitoh, C.-H. Park, Z. X. Shen, P. Villella, N. Hamada, Y. Moritomo, and Y. Tokura, Phys. Rev. Lett. **81**, 192 (1998).

[16] Z. Sun *et al.*, Phys. Rev. Lett. **97**, 056401 (2006).

[17] Z. Sun *et al.*, Phys. Rev. B **78**, 075101 (2008).

[18] Y.-D. Chuang *et al.*, Science **292**, 1509 (2001).

[19] M. W. Kim, H. J. Lee, B. J. Yang, K. H. Kim, Y. Moritomo, J. Yu, and T. W. Noh, Phys. Rev. Lett. **98**, 187201 (2007).

[20] Z. Sun *et al.*, Nat. Phys. **3**, 248 (2007).

[21] N. Mannella *et al.*, Nature (London) **438**, 474 (2005).

[22] S. Rosenkranz (private communication).

[23] R. Saniz, M. R. Norman, and A. J. Freeman, Phys. Rev. Lett. **101**, 236402 (2008).

[24] T. Kimura and Y. Tokura, Annu. Rev. Mater. Sci. **30**, 451 (2000).

[25] A. Koizumi, S. Miyaki, Y. Kakutani, H. Koizumi, N. Hiraoka, K. Makoshi, N. Sakai, K. Hirota, and Y. Murakami, Phys. Rev. Lett. **86**, 5589 (2001).

[26] C. H. Chen, S. Mori, and S.-W. Cheong, Phys. Rev. Lett. **83**, 4792 (1999).

[27] J. C. Loudon, S. Cox, A. J. Williams, J. P. Attfield, P. B. Littlewood, P. A. Midgley, and N. D. Mathur, Phys. Rev. Lett. **94**, 097202 (2005).

[28] S. Larochelle, A. Mehta, N. Kaneko, P. K. Mang, A. F. Panchula, L. Zhou, J. Arthur, and M. Greven, Phys. Rev. Lett. **87**, 095502 (2001).

[29] A. Nucara, P. Maselli, P. Calvani, R. Sopracase, M. Ortolani, G. Gruener, M. Cestelli Guidi, U. Schade, and J. Garcia, Phys. Rev. Lett. **101**, 066407 (2008).

[30] S. Cox *et al.*, Nat. Mater. **7**, 25 (2008).

[31] G. C. Milward *et al.*, Nature (London) **433**, 607 (2005).

[32] F. Ye, S. Chi, J. A. Fernandez-Baca, A. Moreo, E. Dagotto, J. W. Lynn, R. Mathieu, Y. Kaneko, Y. Tokura, and P. Dai, Phys. Rev. Lett. **103**, 167202 (2009).

[33] Z. Jirák *et al.*, J. Magn. Magn. Mater. **53**, 153 (1985).

[34] M. D. Johannes and I. I. Mazin, Phys. Rev. B **77**, 165135 (2008).

[35] F. Weber *et al.*, Nat. Phys. **8**, 798 (2009). This is actually for an $x = 0.40$ sample as data for $x = 0.38$ is lacking.

[36] P. W. Anderson *et al.*, Phys. Rev. **100**, 675 (1955).

[37] P.-G. de Gennes, Phys. Rev. **118**, 141 (1960).